Biol Cybern (2006) 95:519–536
DOI 10.1007/s00422-006-0121-5

ORIGINAL PAPER

Biological Cybernetics

Generation and reshaping of sequences in neural systems

Mikhail I. Rabinovich · Ramón Huerta · Pablo Varona · Valentin S. Afraimovich

Received: 22 August 2006 / Accepted: 18 October 2006 / Published online: 29 November 2006

Abstract The generation of informational sequences and their reorganization or reshaping is one of the most intriguing subjects for both neuroscience and the theory of autonomous intelligent systems. In spite of the diversity of sequential activities of sensory, motor, and cognitive neural systems, they have many similarities from the dynamical point of view. In this review we discus the ideas, models, and mathematical image of sequence generation and reshaping on different levels of the neural hierarchy, i.e., the role of a sensory network dynamics in the generation of a motor program (hunting swimming of marine mollusk *Clione*), olfactory dynamical coding, and sequential learning and decision making. Analysis of these phenomena is based on the winnerless competition principle. The considered models can be a basis for the design of biologically inspired autonomous intelligent systems.

M. I. Rabinovich (✉)· R. Huerta · V. S. Afraimovich
UCSD, Institute for Nonlinear Science,
9500 Gilman Dr., La Jolla, CA, 92093-0402, USA
e-mail: mrabinovich@ucsd.edu

R. Huerta · P. Varona
Grupo de Neurocomputación Biológica (GNB),
Dpto. de Ingeniería Informática, Escuela Politécnica Superior,
Universidad Autónoma de Madrid, 28049 Madrid, Spain
e-mail: rhuerta@ucsd.es

V. S. Afraimovich
Instituto de Investigación en Comunicación Óptica,
UASLP, A. Obregón 64, 78000 San Luis Potosí, SLP, México
e-mail: valentin@cactus.iico.uaslp.mx

P. Varona
e-mail: pablo.varona@uam.es

1 Introduction

Stimulus or information-dependent sequence generation is a critical aspect of most animal and autonomous intelligent system behavior (Lashley 1960; Dominey 2005; Hikosaka et al. 1999; Tanji 2001; Yamauchi and Beer 1994; Worgotter and Porr 2005; Sun and Giles 2001). What is the origin of neural sequences and how is sequential behavior regulated (modulated) by incoming information?

The traditional paradigm for understanding the processing of neural sequences is computation with attractors (Hopfield 1982; Waugh et al. 1990; Hertz et al. 1991; Doboli et al. 2000). This means transformation of a given input, i.e., an initial state inside the basin of attraction of one attractor, to a fixed desired output. However, even in a stationary situation, a sequential behavior is transient, and thus new approaches are needed to describe this kind of neural activity.

Many experimental results allow us to suppose that typical sequential behavior, even at the level of cognition, is the result of competition between different agents or cognitive states. Recently we have introduced a new biologically inspired concept of sequence processing based on the winnerless competition (WLC) principle and on transient but stable heteroclinic sequences (SHSs) (Afraimovich et al. 2004a,b; Rabinovich et al. 2006b). According to the WLC principle, sequential behavior is the result of modulation or reorganization of the intrinsic sequential dynamics of a neural network or a cognitive state machine with WLC by incoming information about the internal or external world.

Stimulus-dependent WLC is a general principle that may be used in different levels of sensory, central, and motor nervous systems, and also in new paradigms of

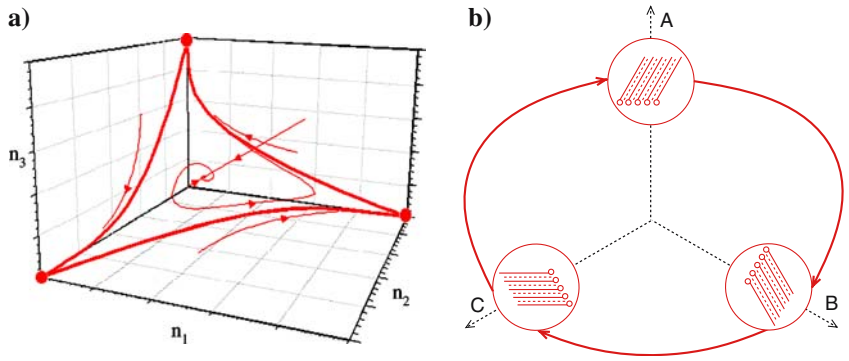

Fig. 1 **a** Phase portrait of autonomous WLC dynamics in a 3-D case. **b** Sequential switching of convection rolls with different orientations. **A**–**C**: amplitudes of convective modes in which the orientation of the rolls is changed 120°

artificial intelligent systems. WLC can be involved in the generation of complex spatiotemporal patterns that control motor activity, sensory encoding, or cognitive functions such as decision making. The origin of a competition can be different at different levels of the system complexity. For small and moderate neural systems like central pattern generators (CPGs), invertebrate sensory systems, or subdivisions of the cortex, competition is a result of the activity of inhibitory interneurons in the network (Rabinovich et al. 2006b; Jefferys et al. 1996; Vida et al. 2006; Nusbaum and Beenhakken 2002). In the whole brain, competitive interaction can be a result of attempts to gain access to processing resources (Fox et al. 2005). The notion of competitive processes in the brain is well represented in the literature. Most relevant is the observation of behavioral competition between task-focused attention and processes that are responsible for stimulus-independent thought (Clark and Fairburn 1997; Giambra 1995; Teasdale et al. 1995). In this review we discuss both inhibitory and population mechanisms of competition. An appropriate set of mathematical models for stimulus-dependent competition phenomena of both origins is based on the generalized Lotka–Volterra equations.

The models describe the cooperative dynamics of an arbitrary number of competitive cognitive states or agents of a different nature. Competition without winners generates robust and reproducible transient or cyclic behavior whose mathematical image is a stable heteroclinic sequence that can be closed or open and finite. A heteroclinic sequence consists of saddle fixed points connected by 1-D unstable separatrices. An incoming informational signal, i.e., a stimulus, is able to reshape the sequence by changing the agent connections or by turning on/off some agents. Thus, the dynamics of WLC networks become sensitive to the incoming message and at the same time remain stable against noise. This is one way to solve the fundamental contradiction between robustness and sensitivity.

Heteroclinic sequences can be robust in the class of perturbed systems preserving the invariance of the sequence in a particular heteroclinic chain. In spite of the fact that SHSs can be robust, they are not so important in practice. This is because the heteroclinic trajectories need an infinite amount of time to reach an invariant set (a saddle point or a saddle cycle, for example). Our interest is in the system dynamics near robust or slightly destroyed, i.e., imperfect, heteroclinic sequences. We name the corresponding image a structurally stable heteroclinic channel (SHC). But before we can understand a realistic rhythmic, chaotic, or transient sequential behavior in a heteroclinic channel, we must begin with a perfect heteroclinic behavior.

The simplest type of heteroclinic sequence is a rhythmic one. This sequence is represented in the phase space by a heteroclinic cycle (Fig. 1a). Heteroclinic cycles have been discovered in many dynamical systems with some level of symmetry. A beautiful experimental example is the convection in a horizontal fluid layer that is rotating around the vertical axis. There is a range of control parameters, associated with Kupper–Lortz instability, where the parallel convection rolls repeatedly switch orientation, each time approximately 120° (Fig. 1b). Such sequential switching of three patterns can be described by the following three-mode model:

$$\begin{aligned}
\dot{a}_1 &= a_1\left[1-(a_1+\rho_{12}a_2+\rho_{13}a_3)\right],\\
\dot{a}_2 &= a_2\left[1-(a_2+\rho_{21}a_1+\rho_{23}a_3)\right],\\
\dot{a}_3 &= a_3\left[1-(a_3+\rho_{31}a_1+\rho_{32}a_2)\right],
\end{aligned}$$

where a_i are the intensities of the convective modes $a_i = |c_i|^2$, and we suppose that the vertical component of the velocity field is in the limit of small amplitudes $u_x = f(z)\sum_{j=1}^{3} c_j(t)\exp\{i\,\mathbf{k}_j\cdot\mathbf{r}\}$, where z is the component of the position vector $\mathbf{r}$ in the vertical direction and $\mathbf{k}_j$ are the wave vectors (Busse and Heikes 1980; Rabinovich et al. 2000).

The nonsymmetry of the coefficients ρ_{ij}, for example $\rho_{12} = \rho_{23} = \rho_{31} \equiv \rho_+ > 1$, $\rho_{21} = \rho_{32} = \rho_{13} \equiv \rho_- < 1$, guarantees the competitive behavior of the discussed dynamical system. The mathematical image of such behavior is a heteroclinic contour in the phase space $a_1(t)$, $a_2(t)$, and $a_3(t)$ (Fig. 1a).

The heteroclinic cycle is associated with intermittent behavior with long periods near each of the saddles (different patterns) followed by a rapid transition along the separatrices (jumping from one pattern to the other). Robust heteroclinic cycles organize the dynamics in a wide range of physical and biological systems. A review of the mathematical results in this subject can be found in Krupa (1997).

Many kinds of perturbations or external forcing (stimuli) are able to destroy a perfect SHS. However, as we will see below, a stable sequential behavior, which keeps the key features of perfect heteroclinic sequences, exists in very realistic situations. In particular, in the cases discussed below, the order of the switching from one state (pattern) to the other is invariant and does not depend on perturbations. In this sense, the heteroclinic channel, i.e., the mathematical image of the vicinity of an imperfect heteroclinic sequence, is a structurally stable dynamical subject (Appendix 1).

Below we concentrate on the discussion of these ideas, results, and possible applications. The mathematical tools are considered just briefly.

2 Stimulus-dependent Clione swimming

Neural sequential dynamics is present at many stages of the sensorimotor transformation. The study of sequential dynamics at the sensory encoding level is an important first step in understanding the transformation from sensory stimuli into motor execution. Small invertebrates are particularly suited for this study as their nervous system is simpler and more directly accessible. The phenomena found in simple neural systems can provide crucial insight into the functioning of more complex networks. As a notable example, here we describe the dual role of the gravity-sensing neural network of the marine mollusc *Clione limacina* due to its stimulus-dependent competitive dynamics in two different behavioral contexts.

2.1 Clione sensory system. Dual role of a gravimetric organ

Clione is a blind planktonic animal that must maintain continuous motor activity in order to keep its preferred head-up orientation in the water. Its motor activity is controlled by the wing CPGs and the tail motoneurons that use signals from its gravity-sensing organ, the statocyst (Panchin et al. 1995). This is a small sphere in which the statolith, a stonelike structure, moves according to the gravitational field. The statolith excites the neuroreceptors that are present in the inner walls of the sphere by pressing down on them. When excited, the receptors, which form a neural network, send signals to the neural systems responsible for wing beating and tail orientation.

During normal swimming, only the statocyst receptor neurons that are excited by the statolith are active (Fig. 2a); this leads to a winner-take-all dynamical mode as a result of the inhibitory connections in the network. (Winner-take-all dynamics is essentially the same as the attractor-based computational idea discussed in the introduction.) However, when *Clione* is searching for its food, a cerebral hunting neuron excites each neuron of the statocyst. Such excitation triggers a WLC between all statocyst neurons characterized by an irregular switching in their activations. These signals are highly correlated with the motor activity, and in vitro recordings show that they participate in the generation of a complex search motion that the animal uses to scan the immediate space until it finds its prey (Levi et al. 2004, 2005). It is important to note that the same sensory network has a different type of dynamics in each behavioral context.

2.2 Dynamical origin of irregular hunting swimming

A six- receptor neural network model with synaptic inhibition has been built to describe the statocyst (Varona et al. 2002b) (Fig. 2). The model uses Lotka–Volterra type dynamics to describe the firing rate of each statocyst receptor neuron:

$$\frac{\mathrm{d}a_i(t)}{\mathrm{d}t} = a_i(t)(\sigma(\boldsymbol{H},\boldsymbol{S}) - \sum_{j=1}^{N} \rho_{ij} a_j(t) + H_i(t)) + S_i(t)\,, \tag{1}$$

where $a_i(t) \geq 0$ is the instantaneous spiking rate of the statocyst neurons, $H_i(t)$ represents the excitatory stimulus from the cerebral hunting interneuron to neuron i, $S_i(t)$ is the action of the statolith on the receptor that is pressing, and ρ_{ij} is a nonsymmetric statocyst network connection matrix. When there is no stimulus from the hunting neuron, $H_i = 0$, or the statolith, $S_i = 0$, then $\sigma(\boldsymbol{H},\boldsymbol{S}) = -1$ and all neurons are silent. When the hunting neuron is active, $H_i \neq 0$, and/or the statolith is pressing one of the receptors, $S_i \neq 0$, $\sigma(\boldsymbol{H},\boldsymbol{S}) = +1$. During normal swimming $H_i = 0$, and the statocyst

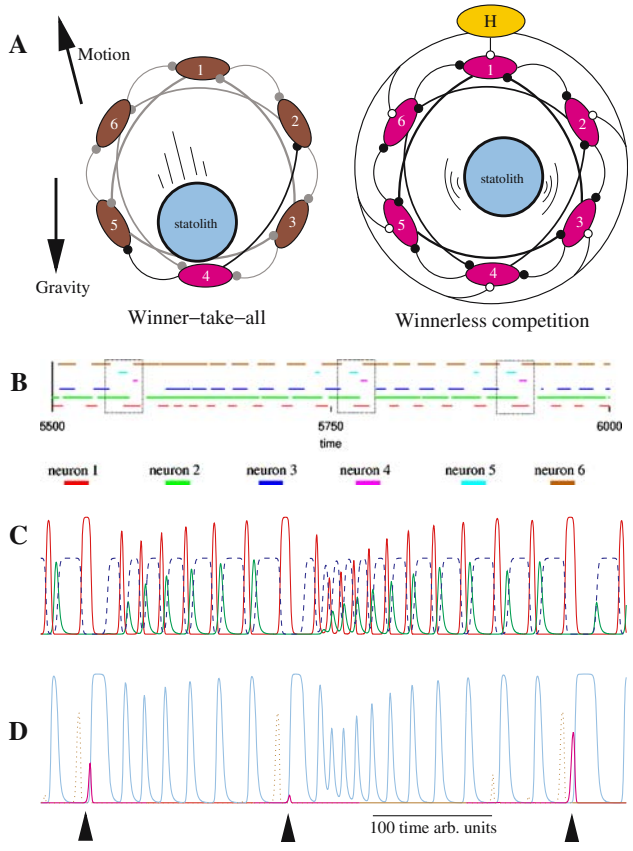

Fig. 2 (Color in online edition) **a** Dual role of a single statocyst, the gravity sensory organ of the mollusc *Clione*. During normal swimming, a stonelike structure, the statolith, hits the mechanoreceptor neurons that react to this excitation. In *Clione*'s hunting behavior, the statocyst receptors receive additional excitation from the cerebral hunting neuron (H) that generates a WLC among them. **b** Chaotic sequential switching displayed by the activity of the statocyst during hunting mode in a model of a six-receptor network. This panel displays the time intervals in which each neuron is active ($a_i > 0.03$). Each neuron is represented by a different color. *Dotted rectangles*: activation sequence locks among units that are active at a given time interval within each network for time windows in which all six neurons are active. **c, d** Irregular switching in the network of six statocyst receptors. Traces represent the instantaneous spiking rate of each neuron a_i (neurons 1, 2, 3 are shown in panel **c**, neurons 4, 5, 6 are shown in **d**. Note that after a neuron is silent for a while, its activity reappears with the same sequence relative to the others (*arrows* and *boxes* in panel **b**

neuron that receives the stimulus from the statolith has the higher spiking rate.

During hunting $H_i \neq 0$, and we assume that the action of the hunting neuron overrides the effect of the statolith, and thus $S_i \approx 0$. A possible set of values for the nonsymmetric connection matrix ρ (which guarantees the WLC dynamics) and the stimuli from the cerebral hunting neuron **H** is:

$$\rho = \begin{pmatrix} 1. & 0. & 5. & 0. & 0. & 1.5 \\ 1.5 & 1. & 0. & 2. & 0. & 0. \\ 0. & 1.5 & 1. & 0. & 5. & 0. \\ 0. & 0. & 1.5 & 1. & 0. & 2. \\ 5. & 0. & 0. & 1.5 & 1. & 0. \\ 0. & 2. & 0. & 0. & 1.5 & 1. \end{pmatrix} \quad \mathbf{H} = \begin{pmatrix} 0.730 \\ 0.123 \\ 0.301 \\ 0.203 \\ 0.458 \\ 0.903 \end{pmatrix}.$$

Too small values in $\rho_{n,n-1}$, $(n = 2, \ldots, 6)$ will make the statocyst network generate a quasiperiodic sequence that would be represented in the state space by an unclosed winding on a torus, which is the direct production of two limit cycles, one in the vicinity of the heteroclinic triangle $1 \to 3 \to 5$ and another one in the vicinity of the triangle $2 \to 4 \to 6$, that are characterized by incommensurate frequencies.

As a result of the competition, the receptors display a highly irregular, in fact chaotic, switching activity. The phase space image of the chaotic dynamics of the statocyst model in this behavioral mode is a strange attractor (the heteroclinic loops in the phase space of (1) become unstable). For six receptors we have shown that the observed dynamical chaos is characterized by two positive Lyapunov exponents (Varona et al. 2002b). The origin of such chaos can be explained as a result of the interaction of two oscillations with incommensurate frequencies. Such interaction destroys the torus and a strange attractor appears in its vicinity.

Panel b in Fig. 2 shows an illustration of the nonsteady switching activity of the receptors. A remarkable phenomenon can be seen in this figure, and it is also pointed out in panels c and d. Although the timing of each activity is irregular, the sequence of activations of the switching among the statocyst receptors is the same at all times for those neurons that are active during a particular time window. Dotted rectangles and arrows in Fig. 2 point out this fact. The activation sequence lock among the statocyst receptor neurons emerges in spite of the highly irregular timing of the switching dynamics and is a feature that can be used for motor coordination.

In this example the WLC is triggered by a constant excitation to all the statocyst receptors ($H_i = c_i$, see details in Varona et al. 2002b). Thus, the stimulus has low information content, yet the network of statocyst receptors can use this activity to generate an information-rich signal with positive Kolmogorov–Sinai entropy. This entropy is equal to the value of the new information encoded in the dynamical motion. The statocyst sensory network is thus multifunctional and can generate a complex spatiotemporal pattern useful for motor coordination even when its dynamics are not evoked by gravity, as happens during hunting (Venaille et al. 2005).

Clione's statocyst network represents an example in which a WLC is generated at a sensory-network level to produce complex motor behavior. The principles used in this multifunctional network could be applied in the design of simple robot search systems. In the next section we illustrate how sequential dynamics is also effective to represent and classify stimuli in a classical sensory context.

3 Sequential dynamics in the olfactory system

3.1 Lessons from locust experiments

In this section we focus our analysis on sequence generation and processing in olfactory networks. In both vertebrates and insects, odor molecules activate a range of odorant receptor types and evoke patterns of activity across defined sets of glomeruli. In the last 10 years, several important experimental results have revealed a key role of spatiotemporal sequential transient dynamics in neuronal computations performed in the olfactory system. Information about the identity and category of odor molecules is encoded as a sequence of dynamical activity patterns.

Odors induce fast oscillations of electrical activity that can be measured as local field potential (LFP) and slow pulsations (~100 ms) that are the result of the intrinsic dynamics at the first stage of the olfactory processing: the antennal lobe (AL) in insects and the olfactory bulb (OB) in vertebrates. Using the zebrafish as a model, Friedrich and Laurent showed that the spatial distribution of active mitral cells changes during the initial phase of a response to a given odor and that the overall pattern becomes informative about the odor identity (Friedrich and Laurent 2002). Concomitantly, subsets of mitral cells phase-lock to the LFP and convey information about odor category. Results from high-resolution activity imaging and computer modeling indicate that these computations rely on inhibitory feedback circuits formed by local interneurons (Bazhenov et al. 2001). The authors in Mazor and Laurent (2005) have analyzed the firing patterns of an ensemble of about 100 projection neurons (PNs) in the AL. They have shown that these neurons exhibit odor-specific dynamic responses and that optimal stimulus separation occurs during the transient phases of the odor representation.

Figure 3 summarizes the architecture of the AL. A specific, i.e., monomolecular, odor generally elicits responses in large ensembles of AL neurons. A comparison of odor-evoked activity from afferents and postsynaptic neurons in the same glomerulus have revealed that second-order neurons display more complex spatiotemporal patterns than their afferents (Wilson et al. 2004). This indicates that odor representation is the result of the interaction of incoming identity information with the intrinsic dynamics of AL.

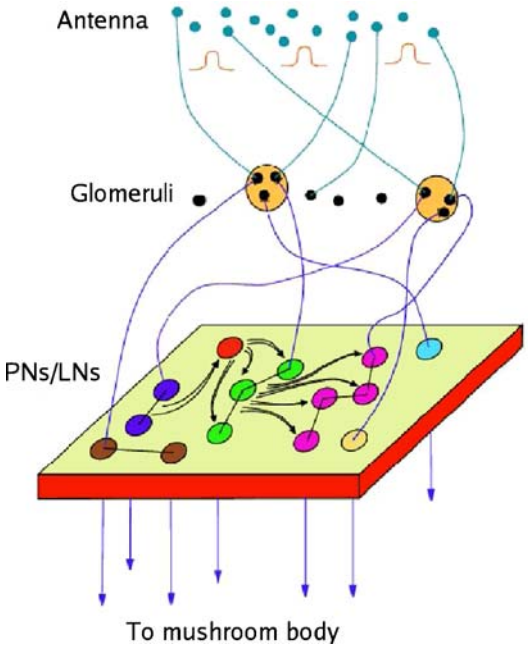

Fig. 3 (Color in online edition) Architecture of antennal lobe (AL). AL is a network of interconnected excitatory PNs and inhibitory local neurons (*LN*). In locust AL, for example, there are 830 PNs and about 300 LNs. PNs are connected with each other through LNs and there are only one-directional connections from PNs to LNs. Both PNs and LNs receive signals from the glomeruli. The mushroom body is the next processing stage for the olfactory signals

Specific odors can be represented by trajectories in the space state of the PN rate activity. Recent results with a Locust AL PN population, stimulated with different odorants and pulse duration between 0.3 and 10 s (Mazor and Laurent 2005), have shown that such trajectories are sequential: first there is a transient part lasting 1–2 s; second there is a fixed point and the trajectory remains in its vicinity for at least 8 s; finally, another transient part lasting a few seconds that corresponds to the moving of the dynamical system to a stable baseline.

Coding of odor information in both insects and vertebrates relies on higher-order neurons in response to short pulses of specific odors (Kenyon cells in locusts). This shows that dynamic, i.e., transient, sequential aspects of the firing patterns of projection neurons indeed support odor discrimination. Sets of Kenyon cells, which generally respond to odors with rare spike events, react selectively during the transient on and off phases of the projection neuron activity, but not when

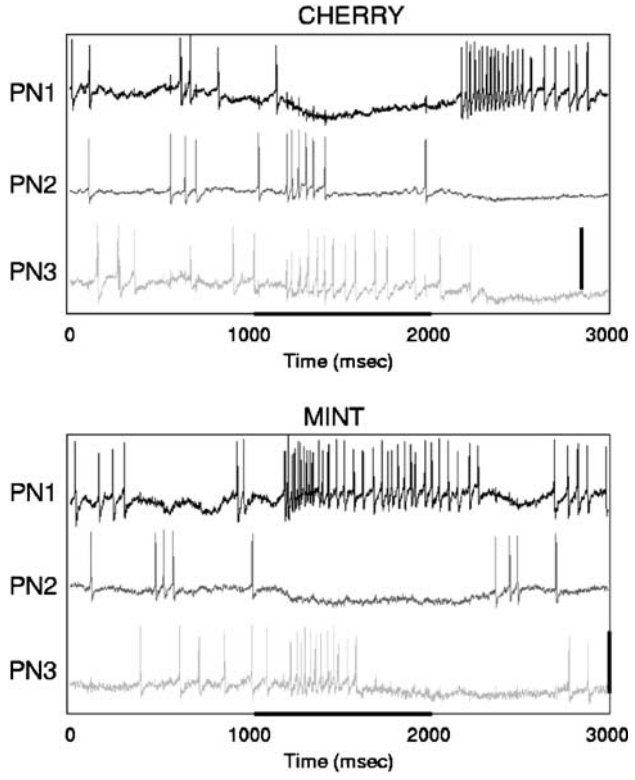

Fig. 4 Temporal patterns produced by three simultaneously sampled PNs in locust antennal lobe when two different odors are presented. *Horizontal bar*: time interval when stimulus was presented Rabinovich et al. 2001

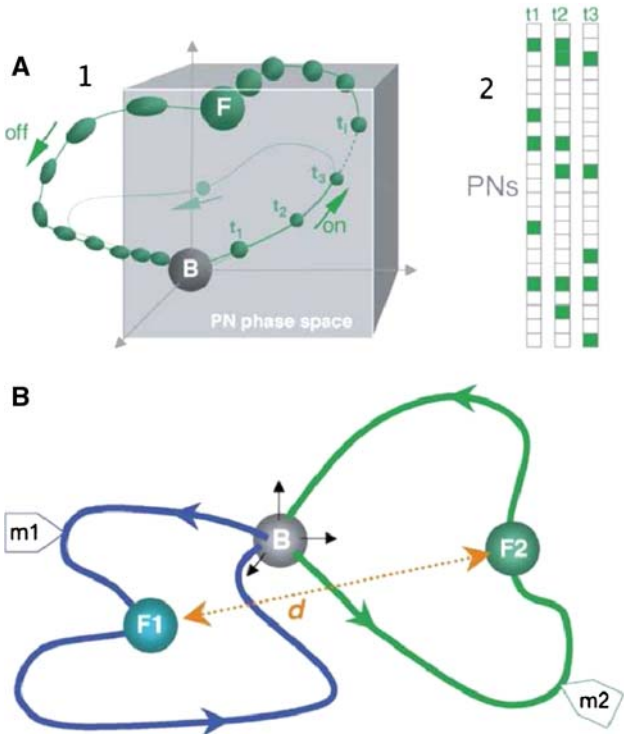

Fig. 5 (Color in online edition) Odor-evoked PN dynamics (modified from Mazor and Laurent 2005). **a**1 Idealized odor trajectory in PN space. *b* baseline; *F* fixed point, t_i times corresponding to one oscillation cycle. During the on transient, synchronization is the highest and most spikes occur within a single 10- to 20-ms period. Activity thus "hops" from one oscillation cycle to the next while the identities of the responding PNs evolve (see **a**2). **a**2 Evolving PN activity underlying trajectory in **a**1. *Squares*: responsive PNs. **b** Idealized trajectories for two different odors. Odor trajectories differ at their fixed points (*F*1 and *F*2) but are maximally distant during the transient response phases (e.g., *m*1 and *m*2)

the highest steady-state firing rate has been reached (Mazor and Laurent 2005).

Figure 4 represents the simultaneously recorded activity of three different projection neurons in the locust AL evoked by two different odors. Despite similar PN activities before stimulus onset (the result of the action of noise), each odor evokes a specific spatiotemporal activity pattern that results from interactions between these and other neurons in the network (Laurent et al. 2001). As a basis for the modeling of the AL dynamics we used these observed features of olfactory processing networks (Rabinovich et al. 2001).

Taking into account the results of the experimental data and knowledge about the anatomy and physiology of the AL, we hypothesize that such olfactory networks form sequential spatiotemporal patterns using the WLC strategy. The experiments indicate the following features of neural encoding: the representation of input (sensory) information (1) uses both identity (or "space") and time, (2) sensitively depends on the stimulus, (3) is based on the transient dynamics of the AL (Fig. 5), (4) is reproducible, and (5) is robust against noise.

In fact, the experiments suggest that (a) the system represents information by transient trajectories, rather than attractors (regular or strange) of the unstimulated system, and (b) a dynamical system that possesses these characteristics should be strongly dissipative so that even a transient trajectory rapidly "forgets" the initial state of the system when the stimulus is activated.

Thus, as recent experiments indicate (Laurent et al. 2001; Mazor and Laurent 2005; Galan et al. 2004), insects represent different odors in some state space by different attractors. However, the real accomplished recognition occurs before the system reaches the fixed point, i.e., classification is based on stable transient trajectories. This provides the animal olfactory system at least two advantages: (1) it is not necessary to wait until the system comes to the vicinity of the attractor (fast recognition) and (2) the distance between transient trajectories that correspond to different odors can be much larger than the distance between attractors (simpler discrimintation).

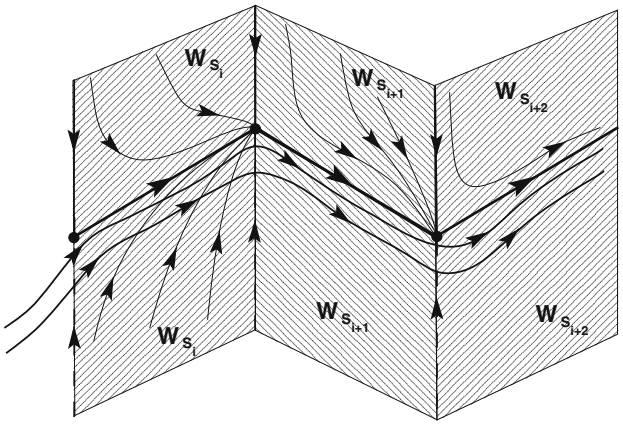

Fig. 6 Stable open heteroclinic sequence in a neural circuit with WLC. W_{s_i} is a stable manifold of the ith saddle fixed point (*heavy dots*). The trajectories in the vicinity of the SHS represent sequences with different timings. The time intervals between switches is proportional to $T \sim |\ln \eta|/\lambda_u$, where λ_u is a positive Lyapunov exponent that characterizes the 1-D unstable separatrices of the saddle points (Stone and Holmes 1990). Modified from Afraimovich et al. (2004a)

3.2 Stable heteroclinic sequence

To build a dynamical model of competitive networks we take into account that PNs compete through the corresponding inhibitory local neurons (LNs). Because of this, the network produces identity-temporal (spatiotemporal) coding in the form of deterministic trajectories moving along a heteroclinic sequence, which consist of 1-D unstable separatrices connecting saddle fixed points in the system's state space (Fig. 6).

The saddle states correspond to specific activities of a neuron or groups of neurons, and the separatrices correspond to the sequential switching from one state to another that can build a limit-cycle, strange attractor (see previous section) or end after the sequential transient activity by a stable fixed point. We can formulate the necessary conditions for the connectivity of a WLC network that must be satisfied in order for the network to exhibit reproducible sequential dynamics along the SHS. As before, we base our analysis on the rate model:

$$\frac{\mathrm{d}\, a_i(t)}{\mathrm{d}t} = a_i(t)\left[\sigma_i(\mathbf{S}^l) - \sum_j^{N^l} \rho_{ij}(\mathbf{S}^l) a_j(t)\right] + \eta_i(t)\,, \qquad (2)$$

where $\eta_i(t)$ is an external Gaussian noise. In this model it is assumed that the stimulus $\mathbf{S}^l$ influences the matrix ρ_{ij} and increments σ_i only in the subnetwork N^l. Each increment σ_i controls the time constant of an initial exponential growth from the resting state $a_i(t) = 0$. In the absence of noise, system (2) has equilibria $A_i = (0, 0, \ldots, \sigma_i, \ldots, 0)$. To assure the SHS, consisting of saddle $A_{i_1}, A_{i_2}, \ldots, A_{i_n}$ and the heteroclinic orbits joining them, is in the phase space of system (2), the following inequalities must be satisfied (for details see (Afraimovich et al. 2004a):

$$\frac{\sigma_{i_{k-1}}}{\sigma_{i_k}} < \rho_{i_{k-1}i_k} < \frac{\sigma_{i_{k-1}}}{\sigma_{i_k}} + 1\,, \qquad (3)$$

$$\frac{\sigma_{i_{k+1}}}{\sigma_{i_k}} - 1 < \rho_{i_{k+1}i_k} < \frac{\sigma_{i_{k+1}}}{\sigma_{i_k}}\,. \qquad (4)$$

It is difficult to satisfy inequalities (3)–(4) in realistic models with random synaptic connections. Is it possible to find reproducible transient sequential behavior such as SHS in complex networks with both random excitatory and inhibitory connections? To answer this question, we discuss here one modeling example described in detail in Huerta and Rabinovich (2004). By using the Wilson–Cowan formalism, we show that it is more likely to find periodic sequential activity (limit cycles) in the regions of the control parameter space where inhibitory and excitatory synapses are slightly out of balance. However, reproducible transient dynamics is more likely found in the regions of parameter space far from balanced excitation and inhibition in the network. In the framework of the model:

$$\mu \frac{\mathrm{d}x_i(t)}{\mathrm{d}t} = \Theta\left(\sum_{j=1}^{N_E} w_{ij}^{EE} x_j(t) - \sum_{j=1}^{N_I} w_{ij}^{EI} y_j(t) + S_i^E\right) - x_i(t), \qquad (5)$$

$$\mu \frac{\mathrm{d}y_i(t)}{\mathrm{d}t} = \Theta\left(\sum_{j=1}^{N_E} w_{ij}^{IE} x_j(t) - \sum_{j=1}^{N_I} w_{ij}^{II} y_j(t) + S_i^I\right) - y_i(t), \qquad (6)$$

where $x_i(t)$ and $y_i(t)$ represent the fraction of active neurons in cluster i of the excitatory and inhibitory population, respectively, N_E and N_I are the numbers of excitatory and inhibitory clusters, the labels E and I are used to denote quantities associated with the excitatory or inhibitory populations, respectively and the external inputs $S_{E,I}$ are instantaneous "kicks" applied to a fraction of the total population at time zero. The gain function is $\Theta(z) = [\tanh((z-b)/\sigma) + 1]/2$, with a threshold $b = 0.1$ below the excitatory and inhibitory synaptic strength of a single connection. The clusters are taken to have very sharp thresholds of excitability by choosing $\sigma = 0.01$. There is a wide range of values that generates similar results. The time scale is set as in Wilson and Cowan (1973), $\mu = 10$ ms. The connectivity matrices w_{ij}^{XY} have entries drawn from a Bernoulli process (Huerta and Rabinovich 2004). The main control parameters in this problem are the *probabilities of connections from population to population*. Figure 7 shows

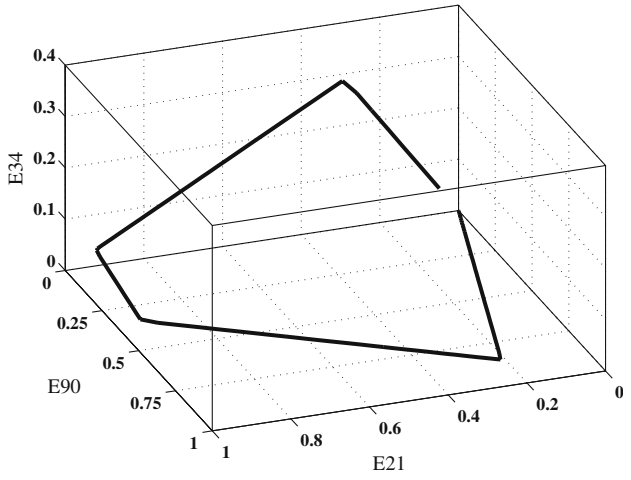

Fig. 7 Five-step reproducible sequence generated in an excitatory-inhibitory network with unbalanced random connections (modified from Huerta and Rabinovich 2004)

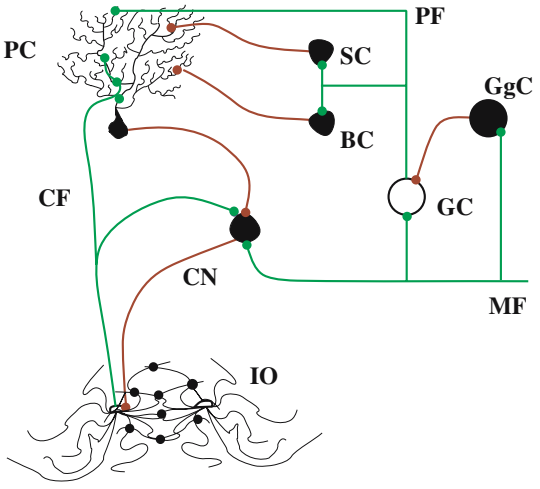

Fig. 8 (Color in online edition) Mammalian cerebellar loop circuits are composed of many inhibitory connections (*red*/*dark traces*). *MF* mossy fibers, *CF* climbing fiber, *PF* parallel fibers, *IO* inferior olive (electrical connections in this population are represented by *black dots*); *CN* cerebellar nuclei, *GC* granule cell, *BC* basket cell, *GgC* Golgi cell, *SC* stellate cell, *PC* Purkinje cell)

a typical example of the sequential dynamics that the system demonstrates when the external input is over.

4 Sequence correction, learning, and decision

We have already discussed that sequential activity in the nervous system can be present at many (if not all) stages of the sensorimotor transformation. Sequential dynamics has several advantageous built-in features to implement tasks such us learning, prediction, error correction, and decision making. In this section we review some important theoretical examples of sequential computation regarding these tasks that are consistent with the available anatomical and physiological data. Section 4.1 reviews these issues in the context of the cerebellar networks. Section 4.2 describes several paradigms for learning sequences. Finally, Sect. 4.3 describes a new framework of sequential decision making (DM).

4.1 Cerebellum spatiotemporal sequential activity

Traditional views of the cerebellum relate it with the acquisition of motor skills, and in particular a leading role in motor control (Llinás and Welsh 1993; Glickstein 1993; Ramnani 2006). The cerebellum is composed of multiple, apparently independent modules, each being a component of a closed anatomical loop that sends and receives projections from specific areas of the cerebral cortex. The cerebellar cortex has a remarkable regular and simple cellular organization that makes it a good model system for theoretical studies. The cerebellar cortex is organized in three layers (Fig. 8), the molecular layer, the Purkinje cell layer, and the granule cell layer. The main inputs to the cerebellar cortex are the mossy fibers and the climbing fibers. Mossy fibers carry sensory and contextual information of multiple modalities. They make specialized excitatory synapses in structures called "glomeruli" with the dendrites of the very numerous granule cells. Granule cell axons form parallel fibers that run transversely in the molecular layer, making excitatory synapses with Purkinje cells. Each Purkinje cell receives thousands of synapses. These synapses are thought to be a major storage site for the information acquired during motor learning. The Purkinje neurons generate the only output from the cerebellar cortex. This output is received by the deep cerebellar nuclei through inhibitory synapses. Each Purkinje cell receives just one climbing fiber input from the inferior olive (IO), but this input is very powerful because it involves several hundred synaptic contacts. The climbing fiber is thought to have a role in "instructing" learning in the cerebellum. The Golgi cell is excited by mossy fibers and granule cells and exercises an inhibitory feedback control upon granule cell activity. Stellate and Basket cells are excited by parallel fibers in order to provide feedforward inhibition to Purkinje cells (Voogd and Glickstein 1998).

Many cerebellar circuits are complex recurrent networks. The large number of inhibitory neurons and the architecture of the cerebellar networks (de Zeeuw et al. 1998) support the generalized WLC mechanism for the encoding and coordination of sequential activity. A widely discussed hypothesis is that the specific circuitry of the IO, cerebellar cortex, and deep cerebellar

nuclei called the "slow loop" (Fig. 8) can serve as a dynamical working memory or as a neuronal clock with a ≈100-ms cycle time, which would make it easy to connect it to behavioral time scales (Kistler and de Zeeuw 2002; Melamed et al. 2004).

From this point of view the cerebellar circuits have an advantageous feature to organize sequential activity: the existence of an intrinsic clock that can time events and serve to compare and coordinate them in different time scales. The IO has been proposed as a system that controls and coordinates different rhythms through the intrinsic oscillatory properties of its neurons and the nature of their electrical interconnections (Llinás and Welsh 1993; de Zeeuw et al. 1998). It has also been implicated in motor learning (Ito 1982) and in comparing tasks of intended and achieved movements as a generator of error signals (Oscarsson 1980). Experimental recordings show that IO cells are electrically coupled and display subthreshold oscillations and spiking activity. Subthreshold oscillations have a relevant role for sequential information processing in the context of a system with extensive electrical coupling. In such systems the spiking activity can be propagated through the network, and, in addition, small differences in hyperpolarized membrane potentials propagate among neighboring cells. IO dynamics has been studied using large-scale network models (Varona et al. 2002a). Both the subthreshold oscillations and the spiking activity, propagated through the gap junctions, contribute to the generation of coherent and coordinated spatiotemporal patterns of organized sequential activity. The patterns arise from the small phase shifts in the quasisynchronized subthreshold oscillations. The occurrence of a spike induces new phase shifts and fast propagating waves that shape the activation sequences and thus the pattern within the quasisynchronized (period locked) subthreshold activity. Coordination properties in this network arise from the subthreshold oscillations that keep a high degree of synchronization due to the extensive electrical connectivity in this network. In the presence of stimuli, different rhythms can be encoded in the spiking activity of the neurons that nevertheless remains constrained to a commensurate value of the subthreshold frequency (Fig. 9). In this context, the climbing fibers to Purkinje cells in the cerebral cortex can carry motor signals beating on the rhythm of the subthreshold oscillations and locally propagated through the precisely timed wavefronts of the IO spiking activity. It is also possible in this system to organize a context-dependent coordination of the spatiotemporal patterns that are coming from different sources. Both these functions can provide, from the commensurality of the different incoming frequencies, a convenient representation of motor rhythms for the next processing levels that is adequate for comparison tasks and also to generate error-correction signals.

A remarkable phenomenon arises in the IO model networks when two particular clusters are present, one with a higher rate of spiking activity than the average population and the other with no spiking activity at all (subthreshold oscillating neurons). In this situation, the wavefronts generated in the cluster with high spiking activity travel to the cluster with intrinsically subthreshold oscillations (Fig. 9, bottom panel). If the excitability of the inferior olive neurons is modulated by the stimulus (in particular the inhibitory connections), this source-sink phenomenon could be used to transport characteristic spatiotemporal patterns from one place of the network to another. The ability to move the wavefronts from one region to another can be an important feature for a system with topology-preserving connections, such as those found in the cerebellar circuits.

An important question regarding motor control by the cerebellum is the following: How can the cerebellum coordinate rhythms with strongly different time scales? Heteroclinic synchronization or coordination (Rabinovich et al. 2006a) of neural rhythms in the cerebellar inhibitory loops can solve this problem, in particular through the transient coordination of SHC activity. This mechanism can also participate in the comparison between the neural representations of intended and achieved movements for error-correction tasks, as these representations can be encoded in different time scales.

Cerebellar circuits have provided inspiration to develop models of timing and prediction for the control of motor movements (Barto et al. 1999; van der Smagt 2000). Robot control architectures have been inspired by the biology of the cerebellum (Collins and Wyeth 1999). In many of these models it is hypothesized that through a learned internal model, the "robot cerebellum" is able to overcome the inherent sensory latency and coordinate fast, accurate movements without the need for complex algorithms. Dynamical approaches like the one presented in this paper can greatly contribute to this effort.

4.2 Learning of sequences

How can neural networks of the nervous system learn meaningful sequences? Sequence learning and memorization, like sequence generation, requires temporal asymmetry in the system. Such asymmetry can be the result of specific properties of the network connections, in particular, the asymmetry of the connections. It can

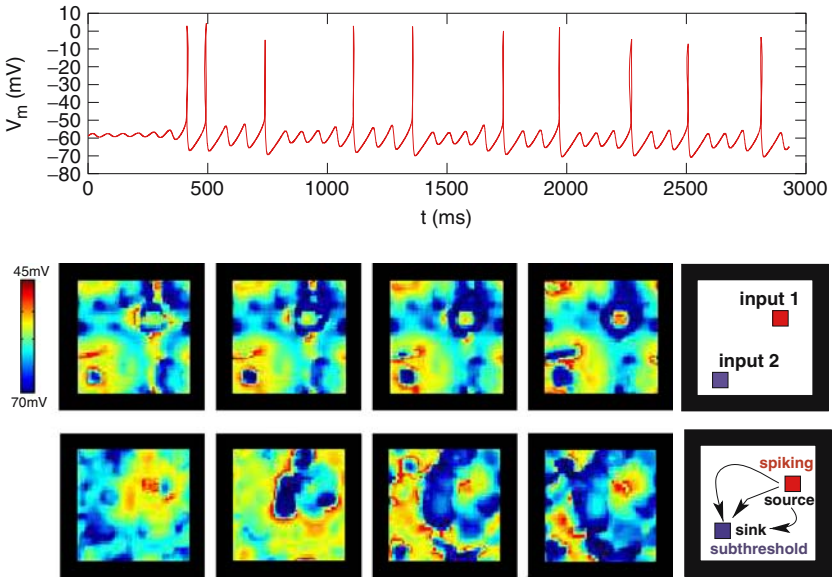

Fig. 9 (Color in online edition) Spatiotemporal patterns of coordinated rhythms induced by stimuli in a model of IO network. *Top panel*: characteristic behavior of a single Hodgkin–Huxley IO model neuron with subthreshold oscillations and spiking activity. Several structures with different frequencies can coexist simultaneously in a commensurate representation of the spiking frequencies of the IO network when several stimuli are present (*middle panel*). Incommensurate stimuli are introduced in the form of current injections in different clusters of the network. (*Panels on right* show position of input clusters.) These current injections induce different spiking frequencies in the neurons. (Colors in these *panels* represent different current injections and thus different spiking frequencies in the input clusters). *Middle panel*: activity of a network of 50 × 50 neurons with two different input clusters. Sequences develop in time from *left* to *right*. Regions with the same color have synchronous behavior. The *color bar* maps the membrane potential. *Red*: spiking neurons (−45 mV is above the firing threshold in the model); *dark blue*: hyperpolarized activity. *Bottom panel*: sink-source phenomena observed when a cluster of model neurons is set to have a high rate of spiking activity while another is set in a subthreshold oscillatory regime. *Right panel*: approximate location of the source (cluster with highly excitable neurons) and the sink (cluster with low excitable neurons). The spiking wavefronts travel from the source to the sink cluster (modified from Varona et al. 2002a)

also be the result of temporal asymmetry in the dynamical features of individual neurons and synapses, or both. The specific dynamical mechanisms of sequence learning depend on the time scale of the sequence that the neural system needs to learn. Learning of fast sequences needs precise synchronization of the spikes or phases of neural waves. For slow sequences, such as autonomous repetitive behavior, it would be preferable to learn the relevant behavioral events that typically occur on the time scale of hundreds of milliseconds or slower and the switching (transitions) between them. Networks whose dynamics are based on WLC are able to engage in such learning.

It is necessary to state clearly one more time that competition is a mechanism that maintains the highest functional level and variety of transient neuronal states, which are essential for the efficiency and stability of neural systems. Nature uses it at all levels of neuronal dynamics from individual neurons (ionic channels competition, synaptic competition) and small neural networks, like CPGs (Selverston et al. 2000), to parts of the brain, like the competition between the basal ganglia and the hippocampus for memory (Poldrack and Packard 2003). At the highest level it can be a competition between brain modes or cognitive states whose dynamics represent such cognitive functions as sequential DM and sequential learning.

Behavioral, functional neuroimaging and neuropsychological studies provide converging evidence for the existence of multiple forms of sequence learning and memory (Bischoff-Grethe et al. 2004; Bapi et al. 2005; Willingham et al. 2002; Doyon et al. 2002; Worgotter and Porr 2005). In particular, several brain structures, i.e., hippocampus, prefrontal cortex, motor cortex, and others, are responsible for the learning of order and timing of behavioral sequences. The level of cooperation of these structures including the leading role of the cerebellum for motor learning is still a subject for investigation (Hazeltine and Ivry 2002).

James A. Anderson, a pioneer in the area of artificial memory, wrote in 1995: “Most memory in humans is associative. That is, an event is linked to another event, so that presentation of the first event gives rise to the linked event.” (Anderson 1995). We think this

is a true statement and we believe it is also true for sequence learning and memorization. Sequence learning and memorization, in fact, is a problem of state or pattern association, i.e., associations between previous and consequent patterns (states). How is it represented mathematically? The SHS that we discussed in detail in Sect. 3.2 is naturally matched to this problem: neighbor saddles correspond to the associated sequential states, and the 1-D unstable separatrix that connects them is an associator.

Here we suggest a dynamical model of cognitive or behavioral sequence learning and memory. This phenomenological model is based on competitive cognitive state dynamics and local learning rules. Cognitive state dynamics, in principle, can describe different parts of the brain like the cerebellum (see above) or the hippocampus (Leibold and Kempter 2006; Seliger et al. 2003), or the cooperation of such parts.

We focus on nonperiodic transient sequences that end when the goal is reached. Here we show that there exist local rules allowing one to drive a cognitive state machine into a prescribed stimulus-dependent sequence. The systems under consideration can be described adequately enough by multidimensional dynamical systems having a SHS. The model that we discuss is based on the competition between different cognitive modes and is similar to the one we discussed with (2). The plasticity of parameters ρ_{ij} in (2), which depend on the activity of the modes a_i, is one of the promising ways to solve the problem of sequence learning and memorization. We show that there exist local rules allowing one to drive a cognitive state machine into a stimulus-prescribed sequence. In contrast to the traditional auto-associative or hetero-associative learning rules (Wang 2000; Lawrence et al. 2005), our local rules for ρ_{ij} are based on the information of the i_kth and the following i_{k+1} states in the sequence. Local learning rules make sequence learning flexible and fast.

4.2.1 Model

We assume that a cognitive state machine is a multidimensional dynamical system having a SHS in the phase space. Every event in a sequence to be remembered corresponds to a saddle equilibrium point. The onset from one event or the next corresponds to a heteroclinic trajectory joining two different saddle points. As before let us consider the system

$$\dot{a}_i = a_i \left[1 - \left(a_i + \sum_{i \neq j}^{N} \rho_{ij} a_j \right) \right] + \eta_i(t)\,, \tag{7}$$

where the coefficients ρ_{ij} are determined by

$$\dot{\rho}_{ij} = \epsilon_j \rho_{ij} \left(\alpha_{ij}(I) a_j - \rho_{ij} \right), \quad i \neq j\,, \tag{8}$$

$$\dot{\epsilon}_j = \gamma \left(\tanh\left((a_j - 1 + c_1)/c_2 + 1 \right) (5 - \epsilon_j) \right) - \epsilon_j\,, \tag{9}$$

where $a_i(t)$ is a cognitive state (it can be brain modes or competitive controllers, see for example Fox et al. 2005), ρ_{ij} denotes the strength of the competitive connection from state j to state i, which is subjected to changes during the learning process, η_i is an external noise, and N is the number of available cognitive states. In (8), $\alpha_{ij}(I) > 0$ is stimulus dependent and contains the training signal, $\epsilon_j > 0$ determines the order of learning, and $c_1 = c_2 = 0.1$ and $\gamma = 0.5$ are parameters of the attractor chosen to lead ρ_{ij} in the target direction. We make use of system (8)–(9) to obtain such values of ρ_{ij} that system (7) will generate a SHS containing dissipative saddle points $S_{j_k} = (0, \ldots, 1, \ldots, 0)$ and the j_kth coordinate equals 1, with $k = 1, \ldots, N_0 \leq N$, with the heteroclinic trajectories joining them. We treat the sequence $\{j_k\} = J$ as the learning signal coming to system (8)–(9), and we use it to determine the values of the parameters ρ_{ij}.

The cognitive state machine learns and memorizes a specific sequence, which is determined by sensory motor input or previous cognitive experience, online. This sequence is formed by a SHS $J = \{j_k\}$ that consists of the saddles $S(j_k)$ joined by heteroclinic trajectories and time intervals that the system spends in the vicinity of the saddle $S(j_k)$. The training signal is given by the parameters α_{ij} that are chosen in the region of the parameter space where a stable heteroclinic trajectory with the proper sequence exist (Appendix 2).

As explained in Appendix 2 there is a region in the space of learning parameters α_{ij} such that the appropriate coefficients $\rho_{ij_1}(t_1), \ldots, \rho_{ij_{N_0}}(t_{N_0})$ can be found as the values of the solutions of system (8)–(9), with suitable initial conditions at times $t_1, \ldots, t_{N_0}$ that are well defined by satisfying the corresponding inequalities.

The ODE for ϵ_j acts as a semaphore to determine what part of the sequence must be learned, when the system is leaving a saddle $S(j_k)$ the corresponding ϵ_j value is reduced while the next ϵ is quickly increased (see 10).

An example of the evolution of the sequence learned by the system is shown in Fig. 10. The learning rules are governed by (8), while (9) determines the time scale of when these rules are to be applied. An example of the time series is shown in Fig. 10. Every time the system leaves a saddle the next epsilon gets activated while the previous one reduces its value sufficiently quickly to 0. In this way the proper order of the sequence is guaranteed.

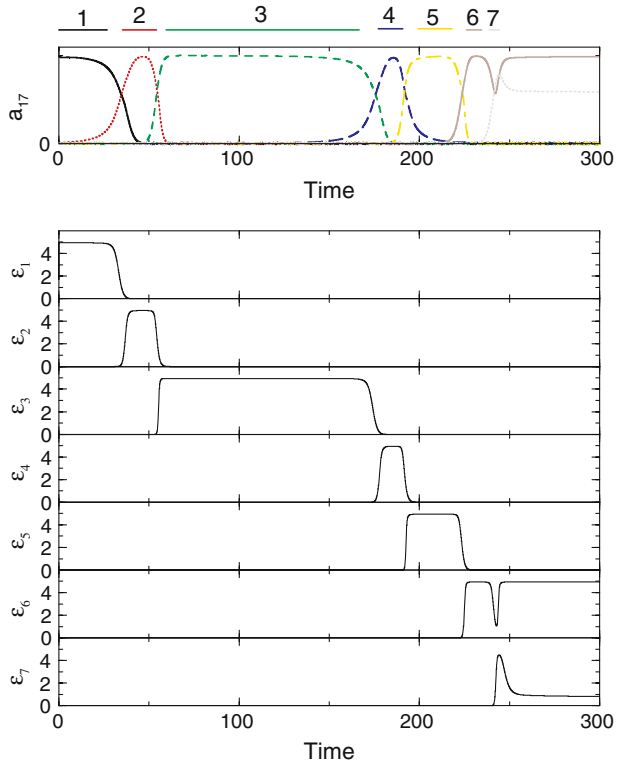

Fig. 10 (Color in online edition) An example of the dynamical process of learning for $N = 7$. We want to teach the system the order of the sequence that, for simplicity's sake, in this case is $1 \to 2 \to 3 \to 4 \to 5 \to 6 \to 7$. The *top panel* illustrates the evolution of each of the variables of system (7) as it travels through each of the saddles. The following *panels* ($\epsilon_1(t)$ to $\epsilon_7(t)$) show the time scale of the learning process of the sequence. The parameter values of time scale of the learning are $c_1 = c_2 = 0.1$ and $\gamma = 0.5$. The ϵ variables are very effective in turning on and off the learning process

4.2.2 Capacity

It is known that 1-D sequences have the highest coding capacity (Rodriguez and Huerta 2004). SHSs are 1-D sequences that are then placed in the optimal coding situation. How many sequences can be learned and stored in the competitive cognitive state machine (CSM) with N states such that their replay can be triggered by an activation of a specific cue pattern (or patterns), i.e., saddles, in a SHS? In Rabinovich et al. (2001) we have estimated the capacity of a closed SHS as $e(N-1)N!$ If the stimulus is changed, another transient trajectory in the vicinity of the new SHS appears for this stimulus. The capacity of the CSM indicates the number of different items, which the CSM may thus encode through its activity. If we satisfy the conditions for one SHS, then we can build another one from it by cutting their length, M, and changing the order of states. Thus, the coding capacity of the SHS can be greatly increased by all the combinations of N by M states.

4.3 Sequential decision making

Animal life is a sequence of choices that are made one at a time. Also, sequential decisions are one of the main goals of autonomous intelligent systems. It is evident that intelligent sequential decision behavior must be stable against noise and at the same time must be sensitive to the information about the new environment to be ready at any step for a fast decision. These requirements are fundamentally contradictory, and traditional models cannot be useful for decision making in sequential activity. However, decision making in dynamical sequential behavior can be based on the generalized WLC principle. The WLC dynamics of a recurrent neural circuit is controlled by the information about the environment and, thus, is able to make the choice between the different learned or genetically determined skills sequentially in time. Here we formulate a new class of models suitable for analyzing sequential decision making (DM).

The decision making system consists of subsystems that (1) formulate the goal, (2) create a decision function, (3) control the parameters of a CSM, and (4) are responsible for the generation of the spatiotemporal patterns of the cognitive states that control the behavior according to the incoming information (I) and DM rules. Here we focus on a dynamical model of the CSM and its parameters, controlled by the decision function and the information about the world, i.e., items (3) and (4).

The natural mathematical image of sequential DM is a stable heteroclinic sequence (SHS) as discussed above. Unstable manifolds in a sequence that connects neighboring saddles in conditions of uncertainty are chosen by the DM function. Suppose the goal of the CSM under investigation is to make active animal life longer. Since the life course can be coded as a sequence of events (Abbott and Tsay 2000), i.e., the number of decisions made in our case, it is reasonable to call the number of decisions made before the cognitive state machine has stopped their activity the "length of life."

4.3.1 Model

Keeping in mind that DM functions are defined algorithmically (see below), we formulated the model (Rabinovich et al. 2006b) in the form of two systems of ODEs. The first one is the set of equations for competitive dynamics of the cognitive states a_i:

$$\dot{a}_i = a_i \left[\sigma_i(I,t) - \left(a_i + \sum_{j \neq i}^{N} \rho_{ij} a_j \right) \right] + \eta_i(t)\,, \tag{10}$$

$$\tau \dot{\sigma}_i = -\frac{\partial U_i(\sigma_i, I)}{\partial \sigma_i}\,. \tag{11}$$

The second system is a gradient system for the control parameters $\sigma(t,I)$. The potential function $U_i(I,\sigma_i)$ has m_k minima

$$\overline{\sigma}_i(I) = \sigma_i^0 + A_i^s(I), \quad s \in \{1,\ldots,m_k\}\,. \tag{12}$$

The initial value $\sigma_i(t_0)$ does not remember the previous history and it is determined by the DM rule in such a way that it chooses the basin of only one minimum. We assume that the characteristic time τ is so small that the dynamics for σ_i can be neglected, and there are only stable equilibrium values, $\overline{\sigma}_i(I)$. Hence we may think that stimulus I acts in such a fashion that at the instants of choice $t_k, k = 1,2,\ldots$, the parameters $\overline{\sigma}_i$ are not unique and may take several values from (12). The times t_k are defined as the instants of arrival of the system to a neighborhood of the fixed points of system (10), and the numbers of possibilities m_k and the values of $\overline{\sigma}_i$ depend on I. Between the instants of choice system (10) evolves according to the values of $\overline{\sigma}_i$ chosen from (12) at time t_k.

We have already mentioned that the mathematical image of the transient dynamics of cognitive states $a_i(t)$ is a SHS with steps that are to be chosen by the DM rule. What happens after the instant of decision? As shown in Afraimovich et al. (2004a), in the absence of noise and $\sigma_i = \overline{\sigma}_i$ system (10) has nontrivial equilibria $S_i = (0,\ldots,0,\overline{\sigma}_i,0,\ldots,0)$. The eigenvalues of the linearized system at S_i are $\lambda_{ji} = \overline{\sigma}_j - \rho_{ji}\overline{\sigma}_i$, $j = 1,\ldots,N, j \neq i$. Depending on the values of λ_{ji} we can find the following possibilities:

1. If all $\lambda_{ji} < 0$, S_i is a stable fixed point, then we say the system reaches the end of its life.
2. If there are at least two values of j, say j_1 and j_2, such that $\lambda_{j_1 i} > 0$ and $\lambda_{j_2 i} > 0$, then we call S_i the "panic state." The system at this point has an infinite number of choices (for heteroclinic orbits in such a situation see Ashwin and Borresen (2005)).
3. If there is only one value $j = j_0$ such that $\lambda_{j_0 i} > 0$ and all others are negative, then the saddle S_i has a 1-D unstable manifold. For the sake of simplicity we will consider only dissipative saddles. Dissipative saddles satisfy the following assumption. Let $\lambda_i^- = \max\{\max_{j \neq j_0, i}\{\lambda_{ji}\}; -\overline{\sigma}_i\}$. Then the number $\nu_i = -\lambda_i^-/\lambda_{j_0 i}$ is called the saddle value (Afraimovich and Hsu 2003). The saddle is dissipative if $\nu_i > 1$, in which case we call S_i the "transient state," and then life continues.

Suppose an initial condition of system (10) is placed in the vicinity of the a_{i_1}-axis, and assume that there is an integer $m_1 > 0$ with possible values of vectors $\underline{\overline{\sigma}} = (\overline{\sigma}_1,\ldots,\overline{\sigma}_N) : \underline{\overline{\sigma}}^1,\ldots,\underline{\overline{\sigma}}^{m_1}$. Before making a decision among them, the system eliminates the following cases based on the intrinsic stimuli. (a) For each value $s \in \{1,\ldots,m_1\}$, the corresponding point S_i is a stable fixed point. (b) For each value $s \in \{1,\ldots,m_1\}$, the point S_i is the panic state. We assume that this case is rare because it is not reproducible and cannot be learned as a new skill by the system. (c) There are values of $s \in \{1,\ldots,m_1\}$ for which S_i is a saddle with the 1-D unstable manifold, yet each of these saddles is nondissipative, i.e., the saddle value $\nu \leq 1$. Case (c) is eliminated because it can lead to instability of the sequential behavior, and the dynamics cannot be reproducible and thus, as in case (b), cannot be learned as memorized skills.

Now we assume that there is at least one value of $s \in \{1,\ldots,m_1\}$, say $s = s'$, such that the corresponding point $S_{i_1}^{s'}$ is the transient state. If such a value is unique, we choose $\underline{\overline{\sigma}} = \underline{\overline{\sigma}}^{s'}$, substitute it into (10), and allow the system to evolve. Since the initial point is close to the a_{i_1}-axis, the point on the corresponding trajectory comes to a small neighborhood of $S_{i_1}^{s'}$, and because $S_{i_1}^{s'}$ is dissipative, it will follow the heteroclinic orbit joining $S_{i_1}^{s'}$ and $S_{j_0} = (0,\ldots,0,\overline{\sigma}_{j_0}^{s'},0,\ldots,0)$ on the plane $\cap_{k \neq i_0, j_0}\{a_k = 0\}$ (Afraimovich et al. 2004a).

4.3.2 Decision-making functions

DM evidently depends on the goal. Let us focus on the goal formulated above with two extreme survival strategies often used by animals (Gigerenzer and Todd 2000). This can be, for example, a risk-aversion DM (stability requirement) or a high-risk DM (minimal time to reach the next decision point).

High-risk DM. Every saddle $S_{i_1}^{s(q)}$ has only one positive increment $\lambda_{j_0 i_1} = \overline{\sigma}_{j_0} - \rho_{j_0 i_1}\overline{\sigma}_{i_1}$, $j_0 = j_0(q)$, $q = 1,\ldots,p$. We choose q_0 in such a way that

$$0 < \lambda_{j_0(q) i_1} < \lambda_{j_0(q_0) i_1}, \quad q \neq q_0\,. \tag{13}$$

In other words, we choose the maximal increment that corresponds to the fastest motion from the saddle S_{i_1} and, therefore, the shortest time to reach the next saddle in SHSs .

Risk-aversion DM. Another way to make a choice is based on stability. For every $q = 1,\ldots,p$, the corre-

sponding saddle value $\nu_{i_1}^q$ is well defined. We choose q_0 in such a way that

$$1 < \nu_{i_1}^q < \nu_{i_1}^{q_0}, \quad q \neq q_0 . \tag{14}$$

After making a decision the system replaces the corresponding value of $\underline{\sigma} = \underline{\sigma}^{s(q_0)}$ in (10) and evolves until the point on the orbit (close to a heteroclinic one) comes to a neighborhood of the saddle $(0,\ldots,0,\overline{\sigma}_{j_0(q_0)}, 0,\ldots,0)$. If this point is fixed as the initial point for the next stage of the process, we denote $j_0(q_0)$ by i_2, taking into account a number m_2 of different vectors $\underline{\sigma}$ and their values. If the saddle S_{i_2} is the transient state, the procedure is repeated again.

4.3.3 Method and parameter values

The model parameters are chosen as in Afraimovich et al. 2004a, where $\overline{\sigma}_i^0$ is taken randomly from the range $\overline{\sigma}_i^0 \in [5,10]$ according to a uniform distribution. Without loss of generality, we set the sequence order from 0 to N in the connectivity matrix so that $\rho_{i-1\,i} = \overline{\sigma}_{i-1}^0/\overline{\sigma}_i^0 + 0.51$ for $i = 2,\ldots,N$, $\rho_{i+1\,i} = \overline{\sigma}_{i+1^0}/\overline{\sigma}_i^0 - 0.5$ for $i = 1,\ldots,N-1$, and $\rho_{ij} = \rho_{j-1\,j} + (\overline{\sigma}_i^0 - \overline{\sigma}_{j-1}^0)/\overline{\sigma}_j^0 + 2$ for $i \notin \{j-1, j, j+1\}$. Finally, each A_i^s is selected randomly from the range $A_i^s \in [-4,9]$ according to a uniform distribution. Then, the possible decisions $\underline{A}^s$ are statistically independent.

System (10) is integrated using a Runge–Kutta method for additive noise (Miguel and Toral 2001). When the trajectory reaches the saddle, S_i, within a ball of radius 0.1, the DM function is applied. We assume that the number of choices at instants t_k is $m_k = M$.

4.3.4 Results of modeling

We calculated the evolution of $a_i(t,t_k)$ by using two antagonistic DM rules, i.e., high-risk and risk-aversion DM. Each DM produces different typical behaviors. A small amount of noise introduces a rich variety of behavior. The noise added to the system is never higher than $\langle \eta(t)\eta(t')\rangle = 10^{-2}\delta(t-t')$.

We calculated the median of the length of life L for different complexity levels of the cognitive states N and number of possible choices M. First we analyze the high-risk DM function (Fig. 12). As shown in Fig. 11, the system can opt to end the sequence soon or wander around until it reaches the last stable fixed point, S_N. It is surprising to find that the system undergoes a phase transition for a given number of choices M when the system size is large enough. For $N = 10$ this phase transition where the system is likely to wander around is not present and it always reaches a stable fixed point. It is also interesting to note that the phase transition point is not strongly

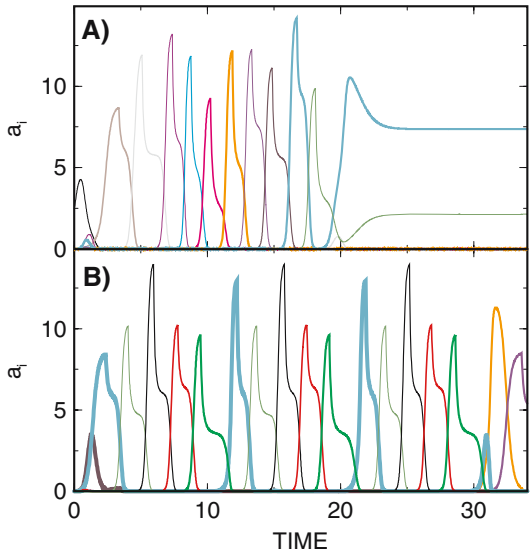

Fig. 11 (Color in online edition) High-risk DM dynamics of a system with $N = 20$ and $M = 5$. **a** Most commonly observed DM behavior. **b** Example of repetitive decisions found in a system with repetitive environment and small percentage of uncertainty. Different tones represent different a_i

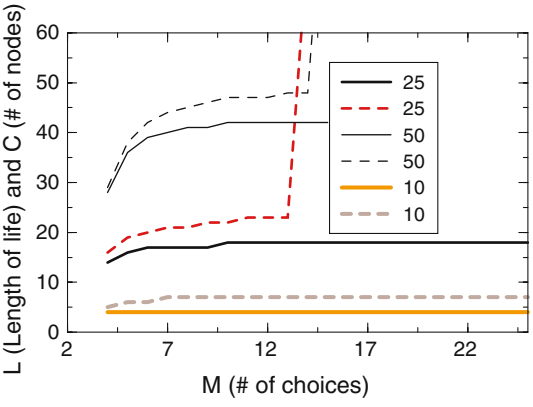

Fig. 12 (Color in online edition) Median of length of life L (*dotted lines*) and median of number of nodes involved in sequence (*solid lines*) vs. number of choices M for CSM with number of cognitive states: $N = 10, 25, 50$

dependent on the number of choices and the number of cognitive states. These simulations were obtained with 10,000 runs for each N and M. High-risk strategies, when the number of choices is sufficiently large, last longer.

The risk-aversion DM rule generates a completely different result than the high-speed DM. First, the system behavior does not depend on the number of available choices M, and, second, the length of the sequence decays exponentially. In fact, having a larger number of states N in the system yields a faster drop in distance to the sequence.

DM is a very diverse function of the cognitive state machine, and it may need different approaches for modeling in different cases. Here we introduced a class of models that describe the uncertainty of the stimulus-dependent sequential behavior as a multivariance of parameters that control the generation of the spatio-temporal patterns responsible for the behavior. We have shown that high-risk decisions are more effective in increasing the longevity of the sequence. Despite considering a simple strategy, this result is supported by recent phycophysical experiments. In particular, macaques consistently take the riskier choice (Mccoy and Platt 2005), and good investors, who are not carried away by emotions, avoid risk-aversion strategies (Shiv et al. 2005). The model proposed here can be easily realized in hardware for use in artificial intelligent systems.

5 Concluding remarks

We can briefly summarize the main ideas discussed in this paper in the following concluding remarks:

1. Throughout the sensorimotor transformation, sequential transient dynamics of neural activity is present, from very early stages of sensory encoding to the final commands involved in motor behavior. Sequential activity is thus generated, transduced, reshaped, coordinated, and executed at all levels of the neural hierarchy. The mathematical image of transient sequential neural activity is a stable heteroclinic sequence or a stable heteroclinic channel. Taking into account many experimental results, in this paper we discussed a mathematical formalism that can describe the observed phenomena. This formalism is based on the WLC principle that can provide both reproducible and adaptive sequential activities.
2. Although the contemporary dynamical approach to brain cognitive functions dates to the early cybernetics era (Ashby 1960), even a decade ago a dynamical approach to cognitive activity such as sequential learning and sequential DM was lacking. However, in the last few years, the situation has changed. In this review we have discussed a new class of models that combines a dynamical description of stable sequential activity with algorithmic rules at the instants of choice. This class of models can be generalized to unify the dynamical description of deterministic steps in the sequence with a statistical description of the steps in uncertainty conditions.
3. As sequential dynamics is involved in high-cognitive tasks such as learning, prediction, error correction, and DM, the existence of a general theory of transient sequential computation is particularly relevant not only for the understanding and description of animal cognitive functions, but also for the design of new paradigms of artificial intelligent systems.

Appendix 1: Structurally stable heteroclinic channel

To prove the structural stability of a heteroclinic channel, let

$$\dot{x} = f(x, \mu)\,, \tag{15}$$

with $\mu \in \Re^m$, be a family of systems having a SHS $\Gamma = \bigcup_{k=1}^{n} S_{i_k} \cup \Gamma_{k,k+1}$ for $\mu = 0$. For small $\mu \neq 0$, system (15) has saddles $S_{i_k}(\mu)$ and their separatrices $\Gamma_{k,k+1}(\mu)$.

Definition *The family* (15) *is said to have a stable heteroclinic channel in a domain* $D_\epsilon \subset O_\epsilon$ (*where* O_ϵ *is the* ϵ*-neighborhood of the origin in* $\Re^m$) *if*

$$Lt_{\mu\to 0,\mu\in D_\epsilon}\left(\bigcup_{k=1}^{n}\Gamma_{k,k+1}(\mu)\right) = \Gamma\,, \tag{16}$$

where Lt is the topological limit, i.e., the set of accumulation points.

If (16) is satisfied, then an orbit of (15) for $\mu \in D_\epsilon$ starting in an ϵ-neighborhood of the first saddle S_{i_1} will follow the saddles $S_{i_2}, S_{i_3}, \ldots, S_{i_n}$ staying in a "channel" (ϵ-neighborhood) consisting of separatrices $\Gamma_{k,k+1}$, $k = 1, \ldots, n$.

Appendix 2: Sequence training

In this appendix we explain the algorithm for training a given sequence $\{j_k\} = J$ in the following system:

$$\dot{a}_i = a_i\left[1 - \left(a_i + \sum_{i\neq j}^{N}\rho_{ij}a_j\right)\right] + \eta_i(t), \tag{17}$$

where a_i is a "rate observable" representing the instantaneous activity (for example, the firing rate) of the ith agent, ρ_{ij} denotes the strength of the competitive connection from agent j to i, and $\eta_i(t)$ is a small external noise. While ρ_{ij} are constants, system (7) in the absence of the noise has equilibria $S_i = (0, \ldots, 1, \ldots, 0)$, where the ith coordinate equals one, and the others are zeroes $i = 1, \ldots, N$. The eigenvalues of the matrix of the system linearized at S_i are (-1) and $\lambda_{ji} = 1 - \rho_{ij}$. The following conditions guarantee that S_i has a 1-D unstable manifold: there is j' such that

$$\lambda_{j'i} > 0, \quad \lambda_{ji} < 0, \ \ j \neq j'. \tag{18}$$

The number $\nu_i = \max_{j\neq j'} \lambda_{ji}/\lambda_{j'i}$ is called the saddle value (Afraimovich et al. 2004a); S_i is a dissipative saddle if $\nu_i > 1$ and nondissipative if $\nu_i < 1$.

According to our problem, the coefficients ρ_{ij} are not constants but variables governed by learning rules. We impose the rules in the form of the following equations:

$$\dot{\rho}_{ij} = \epsilon_j \rho_{ij} \left(\alpha_{ij} a_j - \rho_{ij}\right), \quad i \neq j, \tag{19}$$

where $\alpha_{ij} > 0$ are parameters chosen to lead ρ_{ij} in the way we want (see below), and $\epsilon_j > 0$. Let us simply remark now that if we substitute $a_{i_0} = 1$ and $a_j = 0$ with $j \neq i_0$ into (19), then the equilibrium point of system (19) $\rho_{ii_0} = \alpha_{ii_0}$ will be asymptotically stable.

We want to use system (19) to obtain such constant values of ρ_{ij} that system (17) will generate a SHS containing dissipative saddle points $S_{j_k} = (0,\ldots,1,\ldots,0)$, the j_kth coordinate equals 1, with $k = 1,\ldots,N_0 \leq N$, and heteroclinic trajectories joining them. Given $\{j_k\} = J$, we describe the process of sequential learning as follows.

1st saddle. Substitute $a_{j_1} = 1$, $a_j = 0$, $i \neq j_1$ into (19) and choose the values of α_{jj_1} such that:

(i) $1 - \alpha_{j_2 j_1} > 0, 1 - \alpha_{jj_1} < 0, j \neq j_2, j_1$,
(ii) the inequality

$$1 - \alpha_{j_2 j_1} + max\left\{-1, max_{i\neq j_1, j_2}(1 - \alpha_{ij_1})\right\} < 0$$

is satisfied,
(iii) the condition $1 - \alpha_{j_1 j_2}\alpha_{j_2 j_1} \neq 0$ is satisfied.

Thus if the ρ_{ij}-coordinates of the solution of system (17), (19) are close to the chosen values of α_{ij}, then the conditions above guarantee (Afraimovich et al. 2004a) that (1) the point S_{j_1} is the saddle with the 1-D unstable manifold, (2) it is a dissipative saddle, and (3) there is a heteroclinic trajectory joining S_{j_1} and S_{j_2}. To obtain such values of ρ_{ij}, one can fix the initial conditions $a_{j_1}(0) \approx 1$, $a_j(0) << 1$, $j \neq j_1$, $0 < \rho_{ij}(0) < 1$, and let system (17), (19) evolve until time t_1 such that $\rho_{ij_1}(t_1)$ satisfies the inequalities

$$1 - \rho_{j_2 j_1}(t_1) > 0, \tag{20}$$
$$1 - \rho_{ij_1}(t_1) < 0, \quad i \neq j_1, \tag{21}$$
$$1 - \rho_{j_2 j_1} + \max\left\{-1, max_{i\neq j_1, j_2}(1 - \rho_{ij_1})\right\} < 0, \tag{22}$$
$$1 - \rho_{j_1 j_2}\rho_{j_2 j_1} \neq 0. \tag{23}$$

If such values are found, one has memorized $\rho_{ij_1}(t_1)$ forever and they are substituted into system (17).

2nd saddle. We impose the conditions

$$1 - \alpha_{j_3 j_2} > 0, \tag{24}$$
$$1 - \alpha_{ij_2} < 0, \quad i \neq j_2, \tag{25}$$
$$1 - \alpha_{j_3 j_2} + \max\left\{-1, \max_{i\neq j_2, j_3}(1 - \alpha_{ij_2})\right\} < 0, \tag{26}$$
$$1 - \alpha_{j_2 j_3}\alpha_{j_3 j_2} \neq 0 \tag{27}$$

on the coefficients of system (19), take the initial values $a_i = a_i(t_1)$ and $\rho_{ij} = \rho_{ij}(t_1)$ and allow system (17) and (19) evolve (except for the ρ_{ij_1}-coordinates, which are already found and fixed by the ϵ equation). Since $a_{j_2}(t_1) \approx 1$, $a_j(t_1) << 1$, and $j \neq j_2$, then for some interval of time the ρ_{ij_2}-coordinates of the solutions of system (19) will be attracted to the values α_{ij_2}, so one can expect that there is a value $t = t_2$ such that $|\rho_{ij_2}(t_2) - \alpha_{ij_2}| << 1$ and the inequalities

$$1 - \rho_{j_3 j_2}(t_2) > 0, \tag{28}$$
$$1 - \rho_{ij_2}(t_2) < 0, \quad i \neq j_2, \tag{29}$$
$$1 - \rho_{j_3 j_2} + \max\left\{-1, \max_{i\neq j_2, j_3}(1 - \rho_{ij_2}(t_2))\right\} < 0, \tag{30}$$
$$1 - \rho_{j_2 j_3}(t_2)\rho_{j_3 j_2}(t_2) \neq 0 \tag{31}$$

are satisfied with $a_{j_3}(t_2) \approx 1$, $a_j(t_2) << 1$, and $j \neq j_3$. The values $\rho_{ij_2}(t_2)$ are memorized and substituted into system (17).

***k*th saddle**. Proceeding inductively, on the kth step we impose the conditions

$$1 - \alpha_{j_{k+1} j_k} > 0, \tag{32}$$
$$1 - \alpha_{ij_k} < 0, \quad i \neq j_k,$$
$$1 - \alpha_{j_{k+1} j_k} + max\left\{-1, max_{i\neq j_k, j_{k+1}}(1 - \alpha_{ij_k})\right\} < 0, \tag{33}$$
$$1 - \alpha_{j_k j_{k+1}}\alpha_{j_{k+1} j_k} \neq 0 \tag{34}$$

on the parameters of the system, choose the initial values $a_i = a_i(t_{k-1})$, $\rho_{ij} = \rho_{ij}(t_{k-1})$ (except for $j = j_1,\ldots,j_k$, for which we already found the constant values of ρ_{ij}), and allow system (17) and (19) to evolve until the time t_{k+1} for which $a_{j_{k+1}} \approx 1$, $a_j \approx 0$, and $|\rho_{ij_{k+1}}(t_{k+1}) - \alpha_{ij_{k+1}}| << 1$.

We repeat the procedure until $a(t)$ comes to a neighborhood of the last saddle. To enrich the closeness of $\rho_{ij_k}(t_k)$ to α_{ij_k}, one must be sure that a_{j_k} remains in a neighborhood of 1 for a sufficiently long interval of time for every $k \leq N_0$. This can be achieved by finding suitable constant values of ϵ_i. But a more elegant approach is to allow ϵ_i to evolve in time. We discovered that if the evolution of ϵ_i is governed by the equation

$$\dot{\epsilon}_j = \gamma\left(\tanh\left((a_j - 1 + c_1)/c_2 + 1\right)(5 - \epsilon_j)\right) - \epsilon_j, \tag{35}$$

then the system switches automatically the α_{ij} values to be applied at each stage of the learning procedure. When

it leaves the saddle, the corresponding ϵ tends to 0 while the next ϵ corresponding to the next saddle increases.

References

Abbott A, Tsay A (2000) Sequence analysis and optimal matching methods in sociology: review and prospect. Sociol Methods Res 29:3–33

Afraimovich V, Hsu S-B (2003) Lectures on Chaotic Dynamical Systems. AMS/IP Studies in Advanced Mathematics. American Mathematical Society, Somerville, MA

Afraimovich V, Zhigulin V, Rabinovich M (2004a) On the origin of reproducible sequential activity in neural circuits. Chaos 14:1123–1129

Afraimovich VS, Rabinovich MI, Varona P (2004b) Heteroclinic contours in neural ensembles and the winnerless competition principle. Int J Bifurcat Chaos 14:1195–1208

Anderson J (1995) An introduction to neural networks. MIT Press, Cambridge, MA

Ashby WR (1960) Design for a Brain, 2nd edn. Wiley, New York

Ashwin P, Borresen J (2005) Discrete computation using a perturbed heteroclinic network. Phys Lett A 347:208–214

Bapi R, Pammi VC, Miyapuram K, Ahmed (2005) Investigation of sequence processing: a cognitive and computational neuroscience perspective. Curr Sci 89:1690–1698

Barto AG, Flagg AH, Sitkoff N (1999) A cerebellar model of timing and prediction in the control of reaching. Neural Comput 11:565–594

Bazhenov M, Stopfer M, Rabinovich M, Huerta R, Abarbanel H, Sejnowski T, Laurent G (2001) Model of transient oscillatory synchronization in the locust antennal lobe. Neuron 30:307–309

Bischoff-Grethe A, Goedert KM, Willingham DT, Grafton ST (2004) Neural substrates of response-based sequence learning using fmri. J Cogn Neurosci 16(1):127–138

Busse F, Heikes K (1980) Convenction in a rotating layer: a simple cased of turbulence. Science 208:173–175

Clark D, Fairburn C (eds) (1997) Science and Practice of Cognitive Behavioral Therapy. Oxford University Press, Oxford

Collins D, Wyeth G (1999) Cerebellar control of a line following robot. In: Proceedings of the Australian conference on robotics and automation (ACRA '99) pp 74–79

de Zeeuw CI, Simpson JI, Hoogenaraad CC, Galjart N, Koekkoek SKE, Ruigrok TJH (1998) Microcircuitry and function of the inferior olive. Trends Neurosci 21:391–400

Doboli S, Minai AA, Best P (2000) Latent attractors: a model for context-dependent place representations in the hippocampus. Neural Comput 12:1009–1043

Dominey PF (2005) From sensorimotor sequence to grammatical construction: evidence from simulation and neurophysiology. Adapt Behav 13(4):347–361

Doyon J, Song A, Karni A, Lalonde F, Adams M, Ungerleider L (2002) Experience-dependent changes in cerebellar contributions to motor sequence learning. Proc Natl Acad Sci USA 99:1017–1022

Fox M, Snyder A, Vincent J, Corbetta M, Essen DCV, Raichle M (2005) The human brain is intrinsically organized into dynamic, anticorrelated functional networks. Proc Natl Acad Sci USA 102(27):9673–9678

Friedrich R, Laurent G (2002) Dynamic optimization of odor representations by slow temporal patterning of mitral cell activity. Science 291:889–894

Galan RF, Sachse S, Galizia CG, Herz AVM (2004) Odor-driven attractor dynamics in the antennal lobe allow for simple and rapid olfactory pattern classification. Neural Comput 16:999–1012

Giambra L (1995) A laboratory method for investigating influences on switching attention to task-unrelated imagery and thought. Conscious Cogn 4:1–21

Gigerenzer G, Todd PM (2000) Simple Heuristics That Make Us Smart. Oxford University Press, Oxford

Glickstein M (1993) Motor skills but not cognitive tasks. Trends Neurosci 16:450–451

Hazeltine E, Ivry R (2002) Can we teach the cerebellum new tricks? Science 296:1979–1980

Hertz J, Palmer R, Krogh A (1991) Introduction to the theory of neural computation. Addison-Wesley, Redwood City, CA

Hikosaka Nakahara H, Rand MK, Sakai K, Lu X, Nakamura K, Miyachi S, Doya K (1999) Parallel neural networks for learning sequential procedures. Trends Neurosci 22:464–471

Hopfield JJ (1982) Neural networks and physical systems with emergent collective computational abilities. Proc Natl Acad Sci USA 79:2554–2558

Huerta R, Rabinovich MI (2004) Reproducible sequence generation in random neural ensembles. Phys Rev Lett 93:238104

Ito M (1982) Cerebellar control of the vestibulo-ocular reflex-around the flocculus hypothesis. Annu Rev Neurosci 5:275–296

Jefferys J, Traub R, Whittington M (1996) Neuronal networks for induced "40 hz" rhythms. Trends Neurosci 19:202–208

Kistler WM, de Zeeuw CI (2002) Dynamical working memory and timed responses: the role of reverberating loops in the olivo-cerebellar system. Neural Comput 14:2597–2626

Krupa M (1997) Robust heteroclinic cycles. J Nonlin Sci 7:129–176

Lashley K (1960) The problem of serial order in behavior. In: Beach FA, Hebb DO, Morgan CT, Nissen HW (eds) The Neuropsychology of Lashley. McGraw-Hill, New York, pp 506–521

Laurent G, Stopfer M, Friedrich RW, Rabinovich MI, Abarbanel HDI (2001) Odor encoding as an active, dynamical process: experiments, computation, and theory. Annu Rev Neurosci 24:263–297

Lawrence M, Trappenberg TP, Fine A (2005) A multi-modular associator network for simple temporal sequence learning and generation. In: Proceedings of ESANN'05, Bruges, Belgium, April 2005, pp 423–428

Leibold C, Kempter R (2006) Memory capacity for sequences in a recurrent network with biological constrain. Neural Comput 18:904–941

Levi R, Varona P, Arshavsky YI, Rabinovich MI, Selverston AI (2004) Dual sensory-motor function for a molluskan statocyst network. J Neurophysiol 91:336–345

Levi R, Varona P, Arshavsky YI, Rabinovich MI, Selverston AI (2005) The role of sensory network dynamics in generating a motor program. J Neuroscience 25:9807–9815

Llinás R, Welsh JP (1993) On the cerebellum and motor learning. Curr Opin Neurobiol 3:958

Mazor O, Laurent G (2005) Transient dynamics versus fixed points in odor representations by locust antennal lobe projection neurons. Neuron 48:661–673

Mccoy AN, Platt ML (2005) Risk-sensitive neurons in macaque posterior cingulate cortex. Nat Neurosci 8:1220–1227

Melamed O, Gerstner W, Maas W, Tsodyks M, Markram H (2004) Coding and learning of behavioral sequences. Trends Neurosci 27:11–14

Miguel MS, Toral R (2001) In: Tirapegui E, Martinez J, Tiemann R (eds) Instabilities and Nonequilibrium Structures VI. Kluwer, Dordrecht

Nusbaum MP, Beenhakken MP (2002) A small-system approach to motor pattern generation. Nature 417:343–350

Oscarsson O (1980) Functional organization of olivary projection to cerebellar anterior lobe. In: Courville J, de Montigny C, Lamarre Y (eds) The inferior olivary nucleus. Raven, New York, pp 279–289

Panchin Y, Arshavsky Y, Deliagina T, Popova L, Orlovsky G (1995) Control of locomotion in marine mollusk clione limacina. IX. Neuronal mechanisms of spatial orientation. J Neurophysiol 73:1924–1937

Poldrack A, Packard MG (2003) Competition among multiple memory systems: converging evidence from animal and human brain studies. Neuropsychologia 41:245–251

Rabinovich M, Ezersky A, Weidman P (2000) The dynamics of patterns. World Scientific, Singapore

Rabinovich M, Huerta R, Varona P (2006a) Heteroclinic synchronization: ultra-subharmonic locking. Phys Rev Lett 96:0141001

Rabinovich M, Varona P, Selverston A, Abarbanel H (2006b) Dynamical principles in neuroscience. Rev Modern Phys 78(4):1213

Rabinovich M, Volkovskii A, Lecanda P, Huerta R, Abarbanel HDI, Laurent G (2001) Dynamical encoding by networks of competing neuron groups: winnerless competition. Phys Rev Lett 8706:U149–U151

Ramnani N (2006) The primate cortico-cerebellar system: anatomy and function. Nat Rev Neurosci 7:511–522

Rodriguez F, Huerta R (2004) Analysis of perfect mappings of the stimuli through neural temporal sequences. Neural Netw 17:963–973

Seliger P, Tsimring LS, Rabinovich MI (2003) Dynamics-based sequential memory: Winnerless competition of patterns. Phys Rev E 67:011905

Selverston A, Rabinovich M, Abarbanel H, Elson R, Szncs A, Pinto R, Huerta R, Varona P (2000) Reliable circuits from irregular neurons: a dynamical approach to unterstanding central pattern generators. J Physiol (Paris) 94:357–374

Shiv B, Loewenstein G, Bechara A, Damasio H, Damasio A (2005) Investment behavior and the negative side of emotion. Psychol Sci 16:435–439

Stone E, Holmes P (1990) Random perturbations of heteroclinic attractors. SIAM J Appl Math 50:726–743

Sun R, Giles CL (2001) Sequence learning: from recognition and prediction to sequential decision making. IEEE Intell Syst 16:67–70

Tanji J (2001) Sequential organization of multiple movements: involvement of cortical motor areas. Annu Rev Neurosci 24(1):631–651

Teasdale J, Dritschel B, Taylor M, Proctor L, Lloyd C, Nimmo-Smith I, Baddeley A (1995) Stimulus-independent thought depends on central executive resources. Mem Cognit 23(5):551–559

van der Smagt P (2000) Benchmarking cerebellar control. Robot Auton Syst 32:237–251

Varona P, Aguirre C, Torres JJ, Rabinovich MI, Abarbanel HDI (2002a) Spatiotemporal patterns of network activity in the inferior olive. Neurocomputing 44–46:685–690

Varona P, Rabinovich MI, Selverston AI, Arshavsky YI (2002b) Winnerless competition between sensory neurons generates chaos: a possible mechanism for molluscan hunting behavior. Chaos 12:672–677

Venaille A, Varona P, Rabinovich MI (2005) Synchronization and coordination of sequences in two neural ensembles. Phys Rev E 71:061909

Vida I, Bartos M, Jonas P (2006) Shunting inhibition improves robustness of gamma oscillations in hippocampal interneuron networks by homogenizing firing rates. Neuron 49:8–9

Voogd J, Glickstein M (1998) The anatomy of the cerebellum. Trends Neurosci 21(9):370–375

Wang L (2000) Heteroassociations of spatio temporal sequences with the bidirectional associative memory. IEEE Trans Neural Netw 11:1503–1505

Waugh F, Marcus C, Westervelt R (1990) Fixed-point attractors in analog neural computation. Phys Rev Lett 64:1986–1989

Willingham DB, Salidis J, Gabrieli JD (2002) Direct comparison of neural systems mediating conscious and unconscious skill learning. J Neurophysiol 88:2451–1460

Wilson HR, Cowan JD (1973) A mathematical theory of the functional dynamics of cortical and thalamic nervous tissue. Kybernetik 13:55–80

Wilson R, Turner G, Laurent G (2004) Transformation of olfactory representations in the drosophila antennal lobe. Science 303:366–370

Worgotter F, Porr B (2005) Temporal sequence learning, prediction, and control: a review of different models and their relation to biological mechanisms. Neural Comput 17(2):245–319

Yamauchi BM, Beer RD (1994) Sequential behavior and learning in evolved dynamical neural networks. Adapt Behav 2(3): 219–246